Designing expanded bipyridinium as redox and optical probes for DNA

Emanuela Trovato, Maria Letizia Di Pietro, Antonino Giannetto, Gregory Dupeyre, Philippe Lainé, Francesco Nastasi, Fausto Puntoriero, Sebastiano Campagna

Designing expanded bipyridinium as redox and optical probes for DNA

Received 00th January 20xx,
Accepted 00th January 20xx

DOI: 10.1039/x0xx00000x

Emanuela Trovato,[a] Maria Letizia Di Pietro,*[b] Antonino Giannetto,[b] Gregory Dupeyre,[c] Philippe P. Lainé,*[c] Francesco Nastasi,[b] Fausto Puntoriero*[b] and Sebastiano Campagna[b]

We report on the light-switch behaviour of two *head-to-tail* expanded bipyridinium species as a function of their interaction with calf thymus DNA and polynucleotides. In particular, both DNA and polynucleotides containing exclusively adenine or guanine moieties quench the luminescence of the fused expanded bipyridinium species. This behaviour has been rationalized demonstrating that a *reductive* photoinduced electron transfer process takes place involving both adenine or guanine moieties. The charge separated state so produced recombines in the tens of picoseconds. These results could help on designing new organic substrates for application in DNA probing technology and lab on chip-based sensing systems.

Introduction

The use of intercalating species such as polypyridine metal complexes based on ruthenium, osmium, iridium, platinum,[1] or organic molecules,[2] may be a good strategy for DNA-probing because of their advantages such as chemical stability and reversibility of the redox processes or luminescence-switching. Recently researchers reported the use of dipyridophenazine (DPPZ) Os(II) or Ru(II) complexes as optical and redox probes for real-time methods such as real-time-PCR or PCR-free assay.[3] However, it is difficult to employ these species as electrochemical probes - or combine optical and redox responses - since their relatively high oxidation potential can destroy the species immobilized on the electrode (because of guanine and adenine oxidation). Beside metal complexes, organic species can be hold as optical probes.[2b,2c]

In this vein, pyridinium and bipyridinium salts are among the functional species the most widely used due to their appealing electron-withdrawing and redox features.[4] In fact, among other implementations, these properties make pyridinium entities suitable to be integrated (i) in photochemical molecular devices (PMDs) to manage photoinduced electron transfer (PET) processes,[5] as is the case for artificial multicomponent systems developed for the conversion of solar energy,[5,6] (ii) within supramolecular systems designed as multielectron carriers, such as molecular batteries,[7] or (iii), as redox-active stations in the field of light-powered molecular machines.[8] In addition to their electrophoric behaviour, certain (bi)pyridinium salts have also recently attracted interest as chromophoric and luminophoric subunits.[4n, 4p, 9]

As regards translational implementations, several years ago we studied the interaction between calf-thymus DNA, on the one hand, and both a tetraaryl-pyridinium species, namely the 1*N*-pyridyl-2,4,6-triphenyl-pyridinium (**1**) and its *fused* derivative 9-phenyl-benzo[c]benzo[1,2]quinolizino[3,4,5,6-*ija*]-[1,6]-naphthyridinium (**2**), on the other hand.[10] It was found that the mono-cationic branched compound (**1**), which does not intercalate into double-stranded DNA, was switched to an intercalating agent upon irradiation with UV light (λ = 320 nm) in the presence of dioxygen. This photochemical bis-cyclization (pericondensation) was indeed leading to the formation of the *fused* species (**2**) which, conversely to the branched parent, could intercalate into the DNA double helix. Overall, this is the process we referred to as "*in-situ* DNA intercalation on demand". Here we study the interaction with DNA of *dicationic* species belonging to the family of *head-to-tail* (i.e. 1,4-) expanded bipyridinium compounds, in both their *branched* and *fused* forms i.e. **3** and **4**, respectively (Scheme 1).[4o] From.a.redox.point.of.view,.these.two.species.have.shown .a.completely.different.behaviour.with.respect.to.the.previous. ones,.while.their.luminescent.excited.state.remains.at.relatively. high.energy.4o.In.particular,.they.can.be.reduced.at.lower.poten tial.with.respect.to.the.corresponding.monocationic.species,.so. allowing.the.access.to.more.oxidant.excited.state.

.

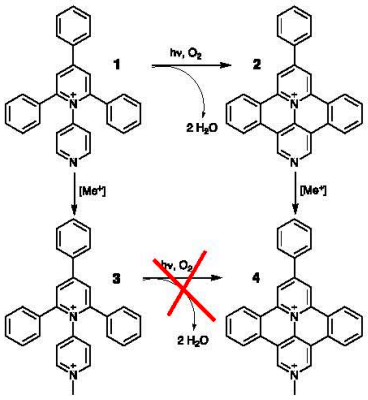

[a] *Chromaleont S.r.l. at Università degli Studi di Messina, Polo Annunziata, Viale Annunziata – 98168 Messina (Italy).*
[b] *Dipartimento di Scienze Chimiche, Biologiche, Farmaceutiche ed Ambientali - ChiBioFarAm - Università di Messina, Viale F. Stagno d'Alcontres 31 - 98166 Messina (Italy).*
[c] *Université de Paris, ITODYS, CNRS, UMR 7086, 15 rue J-A de Baïf F-75013 Paris (France).*
† Footnotes relating to the title and/or authors should appear here.
Electronic Supplementary Information (ESI) available: [details of any supplementary information available should be included here]. See DOI: 10.1039/x0xx00000x

Scheme 1. Molecular structures with labels and synthetic relationship/filiation of here investigated *branched* (**3**) and *fused* (**4**) species.

Results and discussion

The absorption spectrum of **3** in aqueous solution, see Figure 1, exhibits an intense band in the 300÷400 nm region that, on the basis of molar absorption coefficients and band shapes, can be assigned to the lowest energy spin-allowed π-π* transitions. The spectrum recorded for **4**, in the same experimental conditions, is more structured and red-shifted due to the enhanced π-delocalization over the fused polycyclic skeleton of this species (along with existence of a vibronic effect/contribution)[4o] as compared to **3**.

As a first attempt to investigate the interaction of these compounds with polynucleotides, spectrophotometric titrations of **3** and **4** in the presence of incrementally increasing amounts of DNA have been performed (see Figure 1). In both cases, but to sharply different extents, the spectral changes are characterized by hypochromism and a shift to the red of the maxima (bathochromism), as well as isosbestic points. This observation, by far more pronounced for **4** than for **3**, is indicative of a specific interaction between the fused dicationic species and DNA, which is most likely *intercalation*.[11] Moreover, these variations are completely reversible upon addition of sodium chloride, as a confirmation of the non-covalent character of the interaction process.

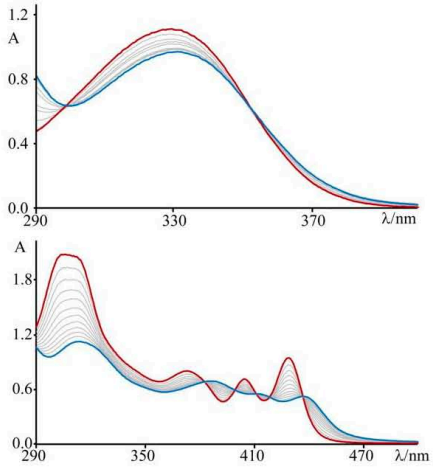

Figure 1. Spectrophotometric titration of (top) **3** (3.5×10^{-5} M) and (bottom) **4** (4.7×10^{-5} M) with DNA at T = 298 K and pH 7 (phosphate buffer, 1×10^{-3} M; NaCl, 2.1×10^{-2} M); starting traces in red and last traces in blue.

To better characterize the interaction of the two pyridinium species with DNA, the melting temperature of DNA in the presence of **3** and **4** have been measured. Intercalation of a compound between the base pairs of the biopolymer stabilizes, in fact, the double helix, thus increasing the temperature at which it melts. The rise of the thermal denaturation temperature of the DNA in the presence of **3** (ΔT_m = 6.5±0.5 K) and **4** (ΔT_m = 14.3±0.5 K) at a 3×10^{-3} M ionic strength value (1×10^{-3} M phosphate buffer at pH 7 and 2×10^{-3} M NaCl) shows that both species stabilize the double helix similarly to what happens in the presence of the well-known reference DNA intercalator ethidium bromide (ΔT_m = 10.1±0.5 K),[12] and much more than $[Pt(en)(py)_2]^{2+}$ (ΔT_m = 2.7±0.5 K), which is unable to intercalate.

Furthermore, intercalation of a species into DNA base pairs causes lengthening and stiffening of the helix which result in an increase of the DNA viscosity. Figure 2 shows the viscosity enhancement induced on rod-like DNA solutions by increasing amounts of **3** and **4** at a 1.1×10^{-2} M ionic strength value, as well as of ethidium bromide and $[Pt(en)(py)_2]^{2+}$ for comparison purposes. As expected,[13] the non-intercalator complex $[Pt(en)(py)_2]^{2+}$ does not produce any significant increase in the viscosity.

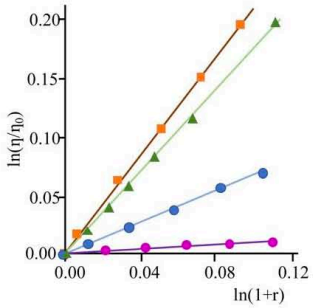

Figure 2. Viscometric titration of DNA (6.0×10^{-4} M) with **3** (blue circles), **4** (orange squares), ethidium bromide (green triangles), and $[Pt(en)(py)_2]^{2+}$ (purple circles) at T = 298 K and pH 7 (phosphate buffer, 1×10^{-3} M; NaCl, 1.0×10^{-2} M). η = reduced viscosity of the DNA solution in the presence of compound, η_0 = reduced viscosity of the DNA solution in the absence of compound, and r = $[compound]_{bound}/[DNA]_{tot}$.

At a 2.2×10^{-2} M ionic strength value (phosphate buffer, 1×10^{-3} M; NaCl, 2.1×10^{-2} M) the resulting binding constant value, K_B (obtained through the McGhee von Hippel equation)[14], is about 7 (± 0.7) × 10^4 M^{-1} for **3** and 1.31 (± 0.1) × 10^6 M^{-1} for **4**, respectively; it thus follows that the species **4** intercalates into DNA with a greater affinity than **3**. This is not at all surprising, since the planar aromatic surface able to intercalate is obviously more extended in the case of the species **4**, in perfect agreement with the results of the viscometric titrations shown in Figure 2.

As far as the luminescence properties are concerned, at room temperature and in buffered solution at pH 7 (phosphate buffer, 1×10^{-3} M; NaCl, 1.0×10^{-2} M), compound **4** exhibits a structured luminescence at 439 nm, with an excited state lifetime of 4.5 ns, while **3** shows a broad emission band centred at 452 nm (τ = 500 ps).

Upon addition of DNA, no significant change in the luminescence of the species **3** is observed until the achievement of a high [DNA]/[**3**] ratio (about 40), for which a very small decrease in emission intensity is detected. This behaviour is assumed to be a consequence of the low affinity of this species towards nucleic acids. On the contrary, addition of DNA aliquots to a solution of **4** produces noteworthy changes of the emission intensity (see Figure 3). The

luminescence, in fact, decreases sharply with increasing nucleic acid concentration, up to a total quenching when the DNA concentration becomes about six-fold that of the bipyridinium species. The species **4** then turns out to be not only sensitive to the presence of the biopolymer, but even to behave as a genuine DNA-sensitive ON/OFF light-switch.

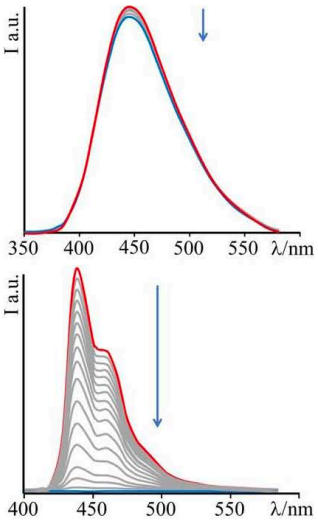

Figure 3. Emission spectral changes of **3** (top) and **4** (bottom) with DNA at T = 298 K and pH 7 (phosphate buffer, 1×10^{-3} M; NaCl, 2.1×10^{-2} M); λ_{exc} = 345 nm and 383 nm for **3** and **4**, respectively.

In order to rationalize the effect of DNA on the luminescence properties of **4**, experiments with synthetic polynucleotides [poly(dA-dT)$_2$] and [poly(dG-dC)$_2$] have been performed (See supplementary material - Figures S1-S2). In both cases a decrease in the luminescence intensity has been observed, until its complete quenching at a [polynucleotide]/[compound] ratio of 6.8 in the case of [poly(dA-dT)$_2$] and of 5.3 for [poly(dG-dC)$_2$].

This behaviour is presumably due to a photo-induced electron transfer process involving guanine or adenine as donors, and the excited state of **4** as the acceptor, in line with usual findings.[3d,15]

The *driving force* associated with these reductive quenching processes can be estimated using the following equation:

$$\Delta G^0_{ET} = (eE_{ox} - eE_{red} - E^{00}) + W \qquad (1)$$

where E_{ox} is the oxidation potential of guanine or adenine (+1.06 V *vs* SCE and +1.20 V *vs* SCE, respectively),[16] E_{red} is the reduction potential of **4** (-0.43 V vs SCE)[4o] and E^{00} is the energy of the excited state of **4** obtained from the highest-energy feature of the 77 K emission spectrum (2.86 eV).[4o] The work term, *W*, is the difference between the Coulombic stabilization energy of reactants and products; its contribution, that slightly reduces the driving force value, is anyway neglected. For **4** the driving force is estimated to amount to -1.37 eV when the donor is the guanine, and to -1.23 eV when adenine is involved. In both cases the processes are thus exergonic. Of note, in the case of **3**, these driving forces are approximatively the same as for **4** (i.e. -1.39 and -1.25 eV for G and A,[4o] respectively), which further substantiates the relevance of the above-invoked assumption that different extents of emission quenching (Figure 3) are indeed related to different binding constants (K_B) of luminophores to DNA.

To get further insights into photochemical processes at work, transient absorption experiments have been performed. Figure 4 shows the pump-probe transient absorption spectra (TAS) of **4** in buffered solution. The initial transient spectrum is characterized by a negative contribution at high energy and a broad absorption centred at around 580 nm. By comparison with the absorption and emission spectra of **4**, the prominent negative signal below 450 nm can be attributed to the bleaching of the ground state absorption, whereas the structured band in the range of 460÷510 nm is ascribed to a stimulated emission contribution. The ground state is recovered, without spectral changes, with an experimental time constant of about 5 ns, in agreement with emission lifetime.

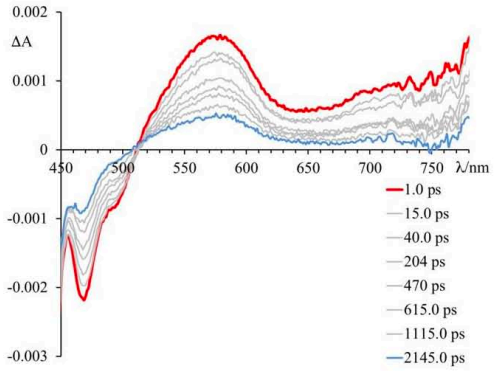

Figure 4. Pump-probe transient absorption spectra (TAS) of **4** in buffered solution at pH 7 (phosphate buffer, 1×10^{-3} M; NaCl, 2.1×10^{-2} M).

Figures 5-7 and Figure S3 gather the TAS of **4** in the presence of DNA, [poly(dG-dC)$_2$] and [poly(dA-dT)$_2$] at a 2.2×10^{-2} M ionic strength value.

As can be observed, in all cases the initial TAS appear to be qualitatively similar. They are characterized by a bleaching at wavelengths lower than 440 nm and intense transient absorption band that extends from 450 nm to 750 nm. On comparing with the absorption spectrum of the ground state, the bleaching at wavelengths lower than 440 nm is attributed to the disappearance of the lowest-energy absorption band.

Contrary to what was observed in TAS matrix of **4** alone (see Figure S3 panel A), in the presence of the polynucleotides the stimulated emission band is no longer observed and, furthermore, the recovery of the ground state takes place in very short times.

In particular, the initial spectrum of the species **4** in the presence of an excess of DNA (see Figure 5, top panel) evolves in approximately 1 ps towards a new species characterized by a contribution in absorption at about 450 nm, which appears simultaneously with an apparent recovery of the bleaching at

435 nm and to a decrease of the transient absorption at 560 nm. An increased absorption at wavelengths longer than 700 nm also appears. This transient species decays, at least biphasically, to the ground state in less than 50 ps.

To better understand this scenario, it is worthwhile analysing in greater detail the results obtained in the presence of the synthetic polynucleotides, so as to discriminate the contributions of individual nucleobases. From a further analysis of Figure 6 it can be seen that, in the presence of [poly(dG-dC)$_2$], the optically formed transient species evolves in 580 fs (± 80 fs) to a new type that exhibits i) a new absorption transient band centred at 450 nm, ii) a recovery of the bleaching at 435 nm and iii) a decrease of the transient absorption intensity at 560 nm. This new species returns to the ground state without further significant changes in about 8.0 ± 0.5 ps. From comparison with the data in literature,[17] in a first approximation, it is possible to assign the absorption band at 450 nm to the formation of the guanine radical cation.

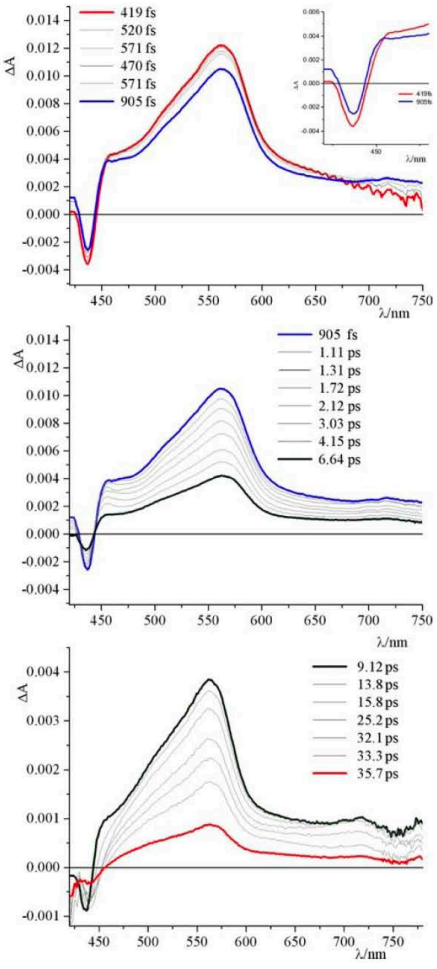

Figure 5. TAS of **4** at pH 7 (phosphate buffer, 1 × 10^{-3} M; NaCl, 2.1 × 10^{-2} M) in the presence of an excess of DNA; λ_{exc} = 400 nm. Top panel report the spectral changes in the early time after excitation, middle panels and bottom panel the evolutions in the following 40 ps. In the inset of the top panel is reported an enlargement of the 420-480 nm spectral region.

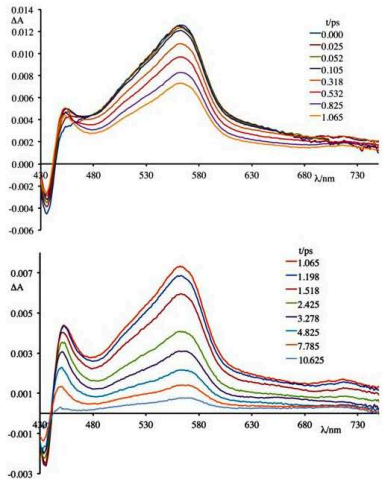

Figure 6. TAS of **4** at pH 7 (phosphate buffer, 1 × 10^{-3} M; NaCl, 2.1 × 10^{-2} M) in the presence of an excess of [poly(dG-dC)$_2$]; λ_{exc} = 400 nm. In the upper panel are reported the spectral changes in the first ps after excitation, in the lower panel the evolutions in the following 11 ps.

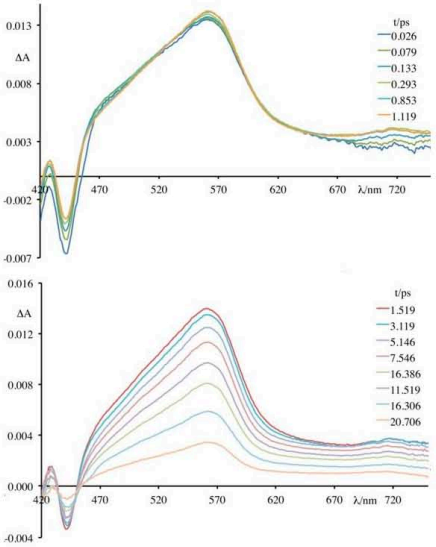

Figure 7. TAS of **4** at pH 7 (phosphate buffer, 1 × 10^{-3} M; NaCl, 2.1 × 10^{-2} M) in the presence of an excess of [poly(dA-dT)$_2$]; λ_{exc} = 400 nm. In the upper panel are reported the spectral changes in the first ps after excitation, in the lower panel the evolutions in the following 21 ps.

Spectroelectrochemical experiments have been conducted on **4**, in acetonitrile solution and $TBAPF_6$ as supporting electrolyte ([$TBAPF_6$] = 5 × 10^{-2} M), upon applying -0.4 V *vs* SCE (Figure 8). At this potential, **4** undergoes a process of reduction which leads to the formation of the mono-cationic radical of **4**.

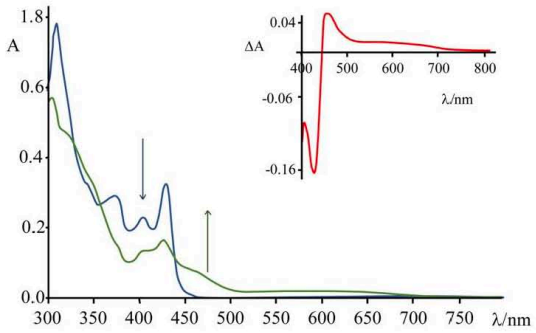

Figure 8. Absorbance spectrum of **4** (blue) in CH_3CN ($[TBAPF_6]$ = 5 × 10^{-2} M) and absorbance spectrum of $\mathbf{4}^{-}$ (green) obtained by applying a potential of -0.4 V *vs* SCE for 60 s. In the inset is reported the difference spectrum.

As can be seen from Figure 8, upon applying -0.4 V for about 60 s, the intensity of the absorption of the species **4** decreases in the region 310÷430 nm and a new band (attributed to the reduced species) centred at 460 nm appears. In the inset of Figure 8 it is possible to observe the calculated difference spectrum, which highlights the appearance of a new band in the region between 440 and 500 nm (with a minor contribution up to 700 nm). Unfortunately, this spectral region is also the one where characteristics of the guanine cation lie, so the proper contributions of the two species cannot be disentangled. The appearance of this absorption feature in the TAS, however, is a strong indication that a charge separated state is formed, involving the excited state of **4** as acceptor and the guanine as donor.

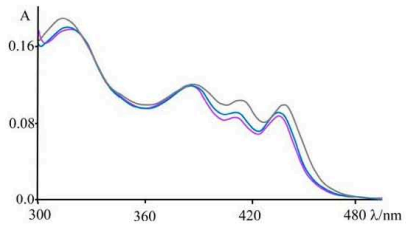

Figure 9. Absorbance spectra of **4** at pH 7 (phosphate buffer, 1 × 10^{-3} M; NaCl, 2.1 × 10^{-2} M) in the presence of an excess of DNA (blue), $[poly(dG\text{-}dC)_2]$ (magenta) and $[poly(dA\text{-}dT)_2]$ (grey); see also Figure 1.

An apparently dissimilar behaviour is observed for **4** in the presence of $[poly(dA\text{-}dT)_2]$ (Figure 7). In fact, differently from what was found in the previous case, the bleaching recorded right after excitation is slightly red-shifted, following the same trend as ground state absorption spectra of the corresponding mixtures (see Figure 9). Unfortunately, as in the case of $[poly(dG\text{-}dC)_2]$, even with $[poly(dA\text{-}dT)_2]$ it is not possible to clearly isolate the transient absorption feature of **4** monoreduced, because its characteristic spectral area is covered by the bleaching. Nevertheless, it is possible to observe some spectral variations, albeit small, that indicate that in a very short time a new species is formed. In these conditions, in fact, **4** shows a first process (in less than 500 fs) which leads to a recovery of bleaching at 443 nm and an increase of the transient absorption at about 550 nm. An increased absorption is also apparent around 700 nm. From the comparison of the absorption spectrum of the monoreduced **4** with that of the adenine cation (which involves a low intensity absorption band at around 550 nm),[15f,18] one can reasonably attribute this spectrum to that of the charge separated species obtained from an electron transfer process from the adenine nucleobase to the excited state of **4** (i.e. **4***). This new species recombines to the ground state in about 25 ps.

Brought together, these findings allow to rationalize the behaviour observed for **4** in the presence of DNA (see Figure 5). In particular, the spectrum formed in about 1 ps is the result of two contributions. In fact, it is possible to assign these spectral variations to the formation of two charge-separated states: one that involves **4*** and the guanine fragments, and one that involves **4*** and the adenine fragments. The species thus formed decays to the ground state bi-exponentially in 6.8 ps and 24 ps. In about 10 ps it is no longer possible to observe the contribution at 450 nm attributed to the guanine radical cation, while the species that involves the adenine radical cation recombines to the ground state in about 24 ps. Therefore, although it is not possible to clearly observe the two contributions that lead to the formation of the mixture of charge-separated states in less than 1 ps, the two different recombination processes leading to the formation of the ground state can be distinguished. The rate constants of the processes of charge recombination can be derived, which amount to 1.4 × 10^{12} s^{-1} in the case of the guanine-based contribution and to 5.9 × 10^{11} s^{-1} in the case of the adenine-based one.

Interestingly, such high rate constants suggest that these photoinduced processes do not imply damage of polynucleotides that would lead to irreversible accumulation of oxidized guanine and/or adenine bases.

Overall, a thorough analysis of the type of the present study can provide a guide for understanding the mechanisms that underpin the processes of charge separation involving DNA. On these bases, new photosensitizers could be designed that are capable either to achieve, if possible as a function of specific sequences of nucleotides, charge-separated states long-live enough to irreversibly damage the DNA, or - as useful for redox-optical devices (e.g. lab on chip devices) - to accelerate the charge recombination in order to obtain an output signal without damaging the DNA. In fact, for this purpose, it is of paramount importance to arrange the competition between the kinetics of charge recombination processes and that of inter-nucleotides hole transfers.[18]

Experimental

Compounds **3** and **4** were synthetized as previously reported.[4o]

Calf thymus DNA, $[poly(dA\text{-}dT)_2]$, and $[poly(dC\text{-}dG)_2]$ were purchased from Sigma Chemical Co. DNA was purified as previously described,[19] $[poly(dA\text{-}dT)_2]$ and $[poly(dC\text{-}dG)_2]$ were

dissolved as received in the phosphate buffer containing the desired amount of NaCl to adjust the ionic strength. Their concentrations, expressed in base pairs, were determined spectrophotometrically using the molar absorptivities:[20] 1.32×10^4 M^{-1} cm^{-1} (258 nm), 1.32×10^4 M^{-1} cm^{-1} (262 nm), and 1.68×10^4 M^{-1} cm^{-1} (254 nm) for DNA, [poly(dA-dT)$_2$], and [poly(dC-dG)$_2$], respectively. All the experiments with DNA and synthetic polynucleotides were carried out at 298 K and pH 7, in a phosphate buffer 1×10^{-3} M and enough NaCl to give the desired ionic strength value.

Absorption spectra were recorded with a JASCO V570 or a Cintra 3030 GBC spectrophotometers. For luminescence spectra, a Jobin Yvon-Spex Fluoromax P spectrofluorimeter was used, equipped with a Hamamatsu R3896 photomultiplier, and the spectra were corrected for photomultiplier response using a program purchased with the fluorimeter. Luminescence lifetimes were determined by time-correlated single-photoncounting (TCSPC) with an Edinburgh OB900 spectrometer (light pulse: Hamamatsu PL2 laser diode, pulse width 59 ps at 408 nm). Experimental uncertainties are as follows: absorption maxima, 2 nm; emission maxima, 5 nm; excited state lifetimes, 10%, unless otherwise stated.

The thermal denaturation temperature of compound–DNA mixtures (1:10) was determined in 1×10^{-3} M phosphate buffer (pH 7) solutions containing the compound (7.8×10^{-6} M) and 2×10^{-3} M NaCl. Melting curves were recorded at 260 nm. The temperature has been increased at a rate of 0.5 K /min by using a GBC Peltier system.

Spectrophotometric titrations were performed by adding to a complex solution [(3.1÷4.7) × 10^{-5} M] successive aliquots of DNA, containing also the complex, in a 10 mm stoppered quartz cell and recording the spectrum after each addition. Data have been reported in the form of Scatchard plots of r/m as a function of m, where r is the binding ratio $[\text{compound}]_{\text{bound}}/[\text{DNA}]_{\text{tot}}$ and m is the concentration of the unbound species. The data were analysed by a nonlinear least-squares fitting program, applied to the McGhee and von Hippel equation.[14] The binding constant, K_B, was determined by the program, using the extinction coefficient of the compounds, the free complex concentration, and the ratio of bound complex per mole of DNA. Extinction coefficient for bound compound was determined by Beer's law plots in the presence of a large excess of DNA.

Viscosity titrations were performed by means of a Cannon-Ubbelhode semimicrodilution viscometer (Series No. 75, Cannon Instrument Co.), thermostatically maintained at 298 K in a water bath. The viscometer contained 2 mL of sonicated DNA solution, in 1×10^{-3} M phosphate buffer (pH = 7) and 1.0×10^{-2} M NaCl. The compound solution ((1.2÷2.0) × 10^{-4} M), containing also DNA (6.0×10^{-4} M) at the same concentration as that in the viscometer, was delivered in increments of 90÷570 μL from a micropipet. Solutions were freed of particulate material by passing them through nylon Acrodisc syringe filters before use. Flow times were measured by hand with a digital stopwatch. Reduced viscosities were calculated by established methods and plotted as $\ln \eta/\eta_0$ against $\ln (1 + r)$ for rodlike DNA (600 base pairs) (η = reduced viscosity of the biopolymer solution in the presence of compound; η_0 = reduced viscosity of the biopolymer solution in the absence of compound; $r = [\text{compound}]_{\text{bound}}/[\text{biopolymer}]_{\text{tot}}$).

Time-resolved transient absorption experiments were performed using a pump–probe setup based on the Spectra-Physics MAI-TAI Ti:sapphire system as the laser source and the Ultrafast Systems Helios spectrometer as the detector. The pump pulse was generated using a Spectra-Physics 800 FP OPA instrument. The probe pulse was obtained by continuum generation on a sapphire plate (spectral range 450÷800 nm). The effective time resolution was around 200 fs, and the temporal chirp over the white-light 450÷750 nm range around 150 fs; the temporal window of the optical delay stage was 0÷3200 ps. In order to cancel out orientation effects on the dynamics, the polarization direction of the linearly polarized probe pulse was set at a magic angle of 54.7° with respect to that of the pump pulse. Please note that all the transient spectra shown in the present paper are chirp corrected. This correction was done by using the pump induced absorption signals themselves in the same conditions (same cuvette, solvent, temperature, stirring frequency...) used for each single experiment. All the time-resolved data were analyzed with the Ultrafast Systems Surface Xplorer Pro software.

UV–vis–NIR spectroelectrochemical measurements were obtained with a SPECAC Omni Cell System: an optically transparent thin-layer electrode (OTTLE) cell with the working Pt-mesh, twinned Ag-wire reference and Pt-mesh auxiliary electrodes melt-sealed into a polyethylene spacer – CaF_2 windows and 0.25 mm path length. The UV–vis–NIR spectra were registered with a JASCO V570 spectrophotometer concurrently applying a potential by using an Autolab multipurpose equipment interfaced to a PC. $TBAPF_6$, (+99%) supporting electrolyte and acetonitrile solvent (anhydrous, 99.8%) were supplied by Aldrich.

Conflicts of interest

There are no conflicts to declare.

Acknowledgements

The Italian Ministero degli Affari Esteri e per la Cooperazione Internazionale (MAECI) is acknowledged by S. C.; M. L. Di P., F. N. and F. P. thanks the University of Messina for the FFABR program.

Notes and references

1 a) A. E. Friedman, J. C. Chambron, J. P. Sauvage, N. J. Turro and J. K. Barton, K. E., *J. Am. Chem. Soc.*, 1990, **112**, 4960; b) E. Trovato, M. L. Di Pietro and F. Puntoriero, *Eur. J. Inorg. Chem.*, 2012, 3984; c) S. Campagna, M. Cavazzini, M. Cusumano, M. L. Di Pietro, A. Giannetto, F. Puntoriero and S. Quici, *Inorg. Chem.*, 2011, **50**, 10667; d) F. Puntoriero, S. Campagna, M. L. Di Pietro, A. Giannetto and M. Cusumano, *Photochem. Photobiol. Sci.*, 2007, **6**, 357.

2 a) S. Conoci, A. Mascali and F. Pappalardo, *RSC Adv.*, 2014, **4**, 2845; b) A. Mancuso, A. Barattucci, P. Bonaccorsi, A. Giannetto, G. La Ganga, M. Musarra-Pizzo, T. M. G. Salerno, A. Santoro, M. T. Sciortino, F. Puntoriero and M. L. Di Pietro, *Chem. Eur. J.*, 2018, **24**, 16972; c) S. Barrois and H.-A. Wagenknecht, *Beilstein J. Org. Chem.*, 2012, **8**, 905.

3 a) T. Defever, M. Druet, D Evrard, D. Marchal and B. Limoges, *Anal. Chem.*, 2011, **83**, 1815; b) S. Petralia, M. E. Castagna, E. Cappello, F. Puntoriero, E. Trovato, A. Gagliano and S. Conoci, Sens. Biosens. Res., 2015, **6**, 90; c) S. Petralia, E. L. Sciuto, M. L. Di Pietro, M. Zimbone, M. G. Grimaldi and S. Conoci, *Analyst*, 2017, **142**, 2090; d) Augustyn, V. C. Pierre and J. K. Barton, Metallointercalators as Probes of DNA Recognition and Reactions; Wiley: New York, 2008; e) X. Qinfeng, D. Jing, M. Xiya, Z. Yanni, L. Chen-chen and Z. Chun-yang, *Analytical Chemistry,* 2019, **91**, 8777.

4 a) V. Balzani, G. Bergamini and P. Ceroni, *Coord. Chem. Rev.*, 2008, **252**, 2456; b) C. Reichardt, *Chem. Rev.*, 1994, **94**, 2319; c) P. Chen and T. Meyer, *J. Chem. Rev.*, 1998, **98**, 1439; d) U. Narang, C. F. Zhao, J. D. Bhawalkar, F. V. Bright and P. N. Prasad, *J. Phys. Chem.*, 1996, **100**, 4521; d) S. R. Marder, J. W. Perry and C. P. Yakymyshyn, *Chem. Mater.*, 1994, **6**, 1137; e) S. R. Marder, J. W. Perry and W. P. Schaefer, *Science*, 1989, **245**, 626; f) B. J. Coe, *Acc. Chem. Res.*, 2006, **39**, 383; g) M. Konstantaki, E. Koudoumas, S. Couris, P. Lainé, E. Amouyal and S. Leach, *J. Phys. Chem. B*, 2001, **105**, 10797; h) S. R. Marder, J. W. Perry, B. G. Tiemann and W. P. Schaefer, *Organometallics*, 1991, **10**, 1896; i) S. Hünig and H. Berneth, *Top. Curr. Chem.*, 1980, **92**, 1; l) C. L. Bird and A. T. Kuhn, *Chem. Soc. Rev.*, 1981, **10**, 49; m) M.-P. Santoni, A. Santoro, T. M. G. Salerno, F. Puntoriero, F. Nastasi, M. L. Di Pietro, M. Galletta and S. Campagna, *ChemPhysChem*, 2015, **15**, 3147; n) J. Fortage, F. Tuyèras, P. Ochsenbein, F. Puntoriero, F. Nastasi, S. Campagna, S. Griveau, F. Bedioui, I. Ciofini and P. P. Lainé, *Chem. Eur. J.*, 2010, **16**, 11047; o) J. Fortage, C. Peltier, F. Nastasi, F. Puntoriero, F. Tuyèras, S. Griveau, F. Bedioui, C. Adamo, I. Ciofini, S. Campagna and P. P. Lainé, *J. Am. Chem. Soc.*, 2010, **132**, 16700; p) C. Peltier, C. Adamo, P. P. Lainé, S. Campagna, F. Puntoriero and I. Ciofini, *J. Phys. Chem. A* **2010**, *114*, 8434-8443; q) J. Fortage, F. Tuyeras, C. Peltier, G. Dupeyre, A. Calborean, F. Bedioui, P. Ochsenbein, F. Puntoriero, S. Campagna, I. Ciofini and P. P. Lainé, *J. Phys. Chem. A*, 2012, **116**, 7880.

5 a) P. P. Lainé, S. Campagna and F. Loiseau, *Coord. Chem. Rev.*, 2008, **252**, 2552; b) J.-P. Sauvage, J.-P. Collin, J.-C. Chambron, S. Guillerez, C. Coudret, V. Balzani, F. Barigelletti, L. De Cola and L. Flamigni, *Chem. Rev.*, 1994, **94**, 993 and references therein; c) V. Balzani, L. Moggi and F. Scandola, in *Supramolecular Photochemistry*, (Ed.: V. Balzani), D. Reidel Publishing Co.: Dordrecht, The Netherlands, 1987, 1; c) V. Balzani and F. Scandola, *in Supramolecular Photochemistry*, Ellis Horwood: Chichester, 1991.

6 a) J. Fortage, G. Dupeyre, F. Tuyèras, V. Marvaud, P. Ochsenbein, I. Ciofini, M. Hromadová, L. Pospísil, A. Arrigo, E. Trovato, F. Puntoriero, P. P. Lainé and S. Campagna, *Inorg. Chem.*, 2013, **52**, 11944; b) J. Fortage, F. Puntoriero, F. Tuyèras, G. Dupeyre, A. Arrigo, I. Ciofini, P. P. Lainé and S. Campagna, *Inorg. Chem.*, 2012, **51**, 5342; c) F. Puntoriero, A. Arrigo, A. Santoro, G. La Ganga, F. Tuyèras, S. Campagna, G. Dupeyre and P. P. Lainé, *Inorg. Chem.*, 2019, **58**, 5807.

7 a) P. Ceroni and M. Venturi, *Aust. J. Chem.*, 2011, **64**, 131; b) M. Marchini, M. Baroncini, G. Bergamini, P. Ceroni, M. D'Angelantonio, P. Franchi, M. Lucarini, F. Negri, T. Szreder and M. Venturi, *Chem. Eur. J.*, 2017, **23**, 6380; c) C. M. Ronconi, J. F. Stoddart, V. Balzani, M. Baroncini, P. Ceroni, C. Giansante and M. Venturi, *Chem. Eur. J.*, 2008, **14**, 8365; d) A. Juris, *Annu. Rep. Prog. Chem., Sect. C*, 2003, **99**, 177; e) R. Toba, J. M. Quintela, C. Peinador, E. Roman and A. E. Kaifer, *Chem. Commun.*, 2002, 1768; f) W. S. Baker, B. I. Lemon and R. M. Crooks, *J. Phys. Chem. B*, 2001, **105**, 8885; g) P. Ceroni and M. Venturi, in *Electrochemistry of Functional Supramolecular Systems* (Eds.: P. Ceroni, A. Credi, M. Venturi), Wiley: Hoboken, NJ, 2010, 145.

8 a) B. Colasson, A. Credi and G. Ragazzon, *Coord. Chem. Rev.*, 2016, **325**, 125; b) W. Sliwa, B. Bachowska and T. Girek, *Curr. Org. Chem.*, 2007, **11**, 497.

9 a) C. Peltier, P. P. Lainé, G. G. Scalmani, M. J. Frisch, C. Adamo and I. Ciofini, *J. Mol. Struct.: THEOCHEM*, 2009, **914**, 94; b) V. Balzani, A. Credi, S. J. Langford, A. Prodi, J. F. Stoddart and M. Venturi, *Supramol. Chem.*, 2001, **13**, 303; c) R. Ballardini, A. Credi, M. T. Gandolfi, C. Giansante, G. Marconi, S. Silvi and M. Venturi, *Inorg. Chim. Acta,* 2007, **360**, 1072.

10 M. L. Di Pietro, F. Puntoriero, F. Tuyèras, P. Ochsenbein, P. P. Lainé and S. Campagna, *Chem. Commun.*, 2010, **46**, 5169.

11 E. C. Long and J. K. Barton, *Acc. Chem. Res.*, 1990, **23**, 271.

12 a) M. J. Waring, *J. Mol. Biol.*, 1965, **13**, 269; b) J. B. LePecq and C. Paoletti, *J. Mol. Biol.*, 1967, **27**, 87.

13 M. Cusumano, M. L. Di Pietro and A. Giannetto, *Inorg. Chem.*, 2006, **45**, 230.

14 J. D. McGhee and P. H. Von Hippel, *J. Mol. Biol.*, 1974, **86**, 469.

15 a) K. E. Erkkila, D. T. Odom and J. K. Barton, *Chem. Rev.*, 1999, **99**, 2777; b) D. García-Fresnadillo, N. Boutonnet, S. Schumm, C. Moucheron, A. Kirsch-De Mesmaeker, E. Defrancq, J. F. Constant and J. Lhomme, *Biophys. J.*, 2002, **82**, 978; c) J. M. Kelly, A. Tossi, D. McConnell and C. OhUigin, *Nucleic Acids Res.*, 1985, **13**, 6017; d) S. Campagna, M. Cavazzini, M. Cusumano, M. L. Di Pietro, A. Giannetto, F. Puntoriero and S. Quici, *Inorg. Chem.*, 2011, **50**, 10667; e) Charge Transfer in DNA: From Mechanism to Applications; Wagenknecht, H. A., Ed.; Wiley: New York, 2005; f) F. D. Lewis, R. M. Young, M. R. Wasielewski, *Acc. Chem. Res.*, 2018, **51**, 1746.

16 S. Steenkßen and S. V. Jovanovic, *J. Am. Chem. Soc.*, 1997, **119**, 617.

17 K. Ohkubo, K. Yukimoto and S. Fukuzumi, *Chem. Commun.*, 2006, 2504.

18 a) C. Dohno, E. D. A. Stemp and J. K. Barton, *J. Am. Chem. Soc.*, 2003, **125**, 9586; b) J. Yoo, S. Delaney, E. D. A. Stemp and J. K. Barton, *J. Am. Chem. Soc.*, 2003, **125**, 6640; c) T. Takada, K. Kawai, S. Tojo and T. Majima, *J. Phys. Chem. B*, 2003, **107**, 14052.

19 M. Cusumano and A. Giannetto, *J. Inorg. Biochem.*, 1997, **65**, 137.

20 C. Hiort, P. Lincoln and B. Norden, *J. Am. Chem. Soc.*, 1993, **115**, 3448.

Designing expanded bipyridinium as redox and optical probes for DNA

Emanuela Trovato, Maria Letizia Di Pietro, Antonino Giannetto, Gregory Dupeyre, Philippe P. Lainé, Francesco Nastasi, Fausto Puntoriero and Sebastiano Campagna

SUPPORTING INFORMATION

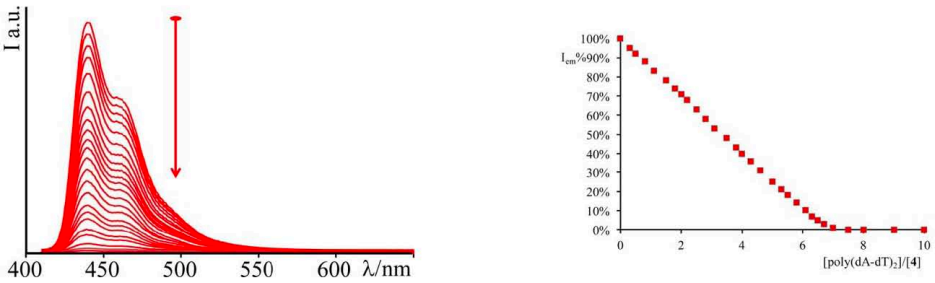

Figure S1. Emission changes of **4** (4.6 x 10^{-6} M) as a function of [poly(dA-dT)$_2$] concentration at T = 298 K and pH 7 (phosphate buffer, 1 x 10^{-3} M; NaCl, 2.1 × 10^{-2} M).

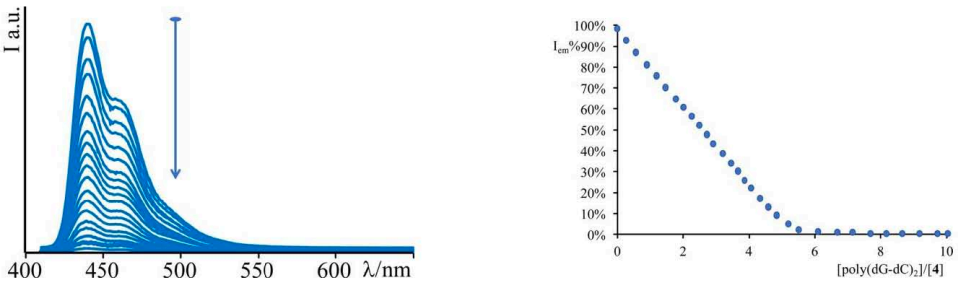

Figure S2. Emission changes of **4** (4.6 x 10^{-6} M) as a function of [poly(dG-dC)$_2$] concentration at T = 298 K and pH 7 (phosphate buffer, 1 x 10^{-3} M; NaCl, 2.1 × 10^{-2} M).

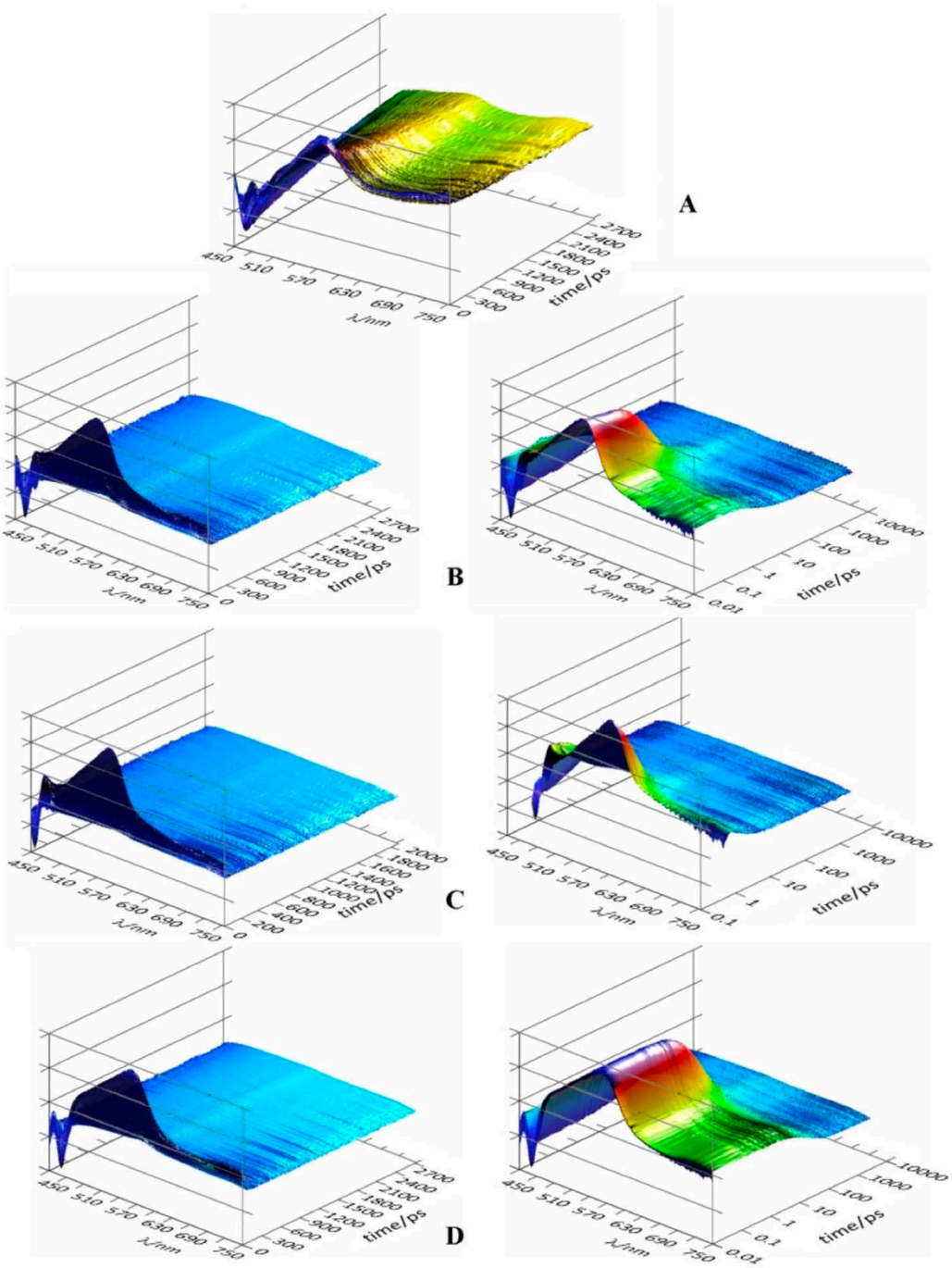

Figure S3. Complete 3D TAS matrices of **4** in phosphate buffer in linear scale vs time (A); **4** in presence of an excess of DNA in linear (B left) and logarithmic (B right) scale; **4** in presence of an excess of [poly(dG-dC)$_2$] in linear (C left) and logarithmic (C right) scale; **4** in presence of an excess of [poly(dA-dT)$_2$] in linear (D left) and logarithmic (D right) scale.